Article

Skin-Like Strain Sensors Enabled by Elastomer Composites for Human–Machine Interfaces

Chunki Yiu [1], **Tsz Hung Wong [1]**, **Yiming Liu [1]**, **Kuanming Yao [1]**, **Ling Zhao [1]**, **Dengfeng Li [1]**, **Zhao Hai [1]**, **Huanxi Zheng [2]**, **Zuankai Wang [2]** and **Xinge Yu [1,***]

[1] Department of Biomedical Engineering, City University of Hong Kong, Hong Kong 999077, China; chunkiyiu2-c@my.cityu.edu.hk (C.Y.); thwong247-c@my.cityu.edu.hk (T.H.W.); lyiming2-c@my.cityu.edu.hk (Y.L.); km.Yao@my.cityu.edu.hk (K.Y.); lingzhao3-c@my.cityu.edu.hk (L.Z.); dengfli2@cityu.edu.hk (D.L.); zhaohai2-c@my.cityu.edu.hk (Z.H.)

[2] Department of Mechanical Engineering, City University of Hong Kong, Hong Kong 999077, China; huanzheng4-c@my.cityu.edu.hk (H.Z.); zuanwang@cityu.edu.hk (Z.W.)

* Correspondence: xingeyu@cityu.edu.hk

check for updates

Abstract: Flexible electronics exhibit tremendous potential applications in biosensing and human–machine interfaces for their outstanding mechanical performance and excellent electrical characteristics. In this work, we introduce a soft, skin-integrated strain sensor enabled by a ternary elastomer composite of graphene/carbon nanotube (CNT)/Ecoflex, providing a low-cost skin-like platform for conversion of mechanical motion to electricity and sensing of human activities. The device exhibits high sensitivity (the absolute value of the resistance change rate under a testing strain level, 26) and good mechanical stability (surviving ~hundreds of cycles of repeated stretching). Due to the advanced mechanical design of the metallic electrode, the strain sensor shows excellent mechanical tolerance to pressing, bending, twisting, and stretching. The flexible sensor can be directly mounted onto human skin for detecting mechanical motion, exhibiting its great potential in wearable electronics and human–machine interfaces.

Keywords: flexible electronics; skin-integrated electronics; strain sensors; graphene; CNT

1. Introduction

Thin, soft, and skin-integrated electronics have attracted extensive attention in the field of biomedical engineering [1–4], owing to their advantages of being multifunctional, wearable [5–8], and flexible [9,10]. They have shown their great potential in various applications, including wearable electronics [11–13], human–machine interfaces [14–16], gaseous monitoring [17,18], and healthcare monitoring [19,20]. The key of developing this kind of electronics is exploring flexile/stretchable sensors with high sensitivity and stability that can accurately detect signals such as strain, temperature, and flows [4,21–24]. In the past decades, extensive efforts have been made to develop flexible strain sensors for continuously monitoring of human health status [25,26]. One successful example of exploring soft strain sensors is adopting intrinsically flexible or stretchable materials serving as the functional layer that exhibits great electrical conductivity [27,28]. Graphene, a two-dimensional material, has outstanding electrical properties that has been used in strain sensors [29–31]. However, due to the intrinsic brittle nature, graphene-based strains sensor encounters a limitation of low stretchability (maximum $\varepsilon = 5\%$) [9,21,32–35]. Similar to graphene, carbon nanotube (CNT) is also an outstanding material for electronic devices [36–40]. It shows great mechanical properties due to its small-sized and ultimate fibril structures that has been reported in various kinds of sensors [36,41]. Nevertheless, the CNT-based strain sensors are limited with their low sensitivity and poor restorability [38]. Combing these conductive nanostructures with elastomer such as

polydimethylsiloxane (PDMS) enables intrinsically stretchable stain sensors [32,42]. However, considering the using of such composite for flexible sensors electronics and practical applications, several challenges, such as integration complexity, flexible circuit design, long-term stability, and cost issues remain. Table S1 provide the typical performances of recently reported strain sensors based on piezoresistance.

Here, we present a skin-integrated strain sensor based on graphene/CNT/Ecoflex via a simple fabrication process and low mass production cost. The reported strain sensor exploits intrinsically stretchable piezoresistive elastomer as sensing pixels by blending graphene and CNT nanoparticles with Ecoflex. One step screen-printing of the piezoresistive elastomer on the preformed in-plane electrodes coated soft substrate forms the strain sensor with high sensitivity and excellent stability. Due to its simple structure and flexible functional material, it owns the properties of softness, ultrathin thickness, 0.64 mm, and lightweight, ~0.27 g/cm^2, that could be stretched and compressed along any directions. It is wearable that can be tightly mounted onto the epidermis of the human body for stable signal measurement. Besides, the strain sensors could capture the signal not only at static state but also at the moment of stretching status. The sensors were integrated into circuit to demonstrate the applications in human–machine interfaces, where the strain sensors were mounted on a human hand for imitating motions and controlling a robotic hand. Rapid and precise imitations of different gestures ("tick", "eight", "yeah" and "okay") were realized for this system. The soft sensors and system show great potential in machine control and offers a new strategy for real-time human–machine interfaces.

2. Experimental Section

2.1. Fabrication of the Graphene/CNT/Ecoflex Composite

Graphene powder (average thickness of 1.75 nm; purity >99 wt.%.) and CNT (diameter, 10–20 nm; length, 10–30 μm) were purchased from Suzhou Hengzhu Graphite Technology Co., Ltd., Suzhou, Jiangsu, China. Ecoflex 00-30 was purchased from Smooth-On, Inc., Macungie, PA, USA. Graphene (0.1 g), CNT (0.6 g), and Ecoflex (34 g; A:B, 1:1) were poured into a speed mixer at the speed of 500 rpm for 1 h to form the rubbery precursors. Then, the mixtures were transferred into an agate mortar and, subsequently, ground for 1 h at room temperature. After full dispersion, the graphene/CNT/Ecoflex composite was poured into marked beakers for film casting.

2.2. Assembly of the Piezoelectric Rubbery Devices

The fabrication started on a quartz glass, which was first sequentially cleaned by acetone, alcohol, and deionized water (DI water). A thin sacrificial layer (liquid soap) was spin coated on the glass sheet for later releasing the device. Then, spin-coating of a thin PDMS film (0.17 mm) was done at 600 rpm for 30 s, and further, it was baked at 110 °C for 5 min. To ensure enough adhesion strength between the copper film and PDMS substrate, another ultrathin PDMS film was spread over the cured PDMS substrate before attaching copper film (thickness, 6 μm) on it. After smoothly attaching copper film onto the PDMS substrate, the sample was cured at 110 °C for 5 min and then, patterned by photolithography and etching, yielding metal traces in the desired geometries. Here, a positive photoresist (PR, AZ 4620, AZ Electronic Materials, Ulm, Germany) was spin-coated at 3000 rpm for 30 s, soft baked on a hot plate at 110 °C for 5 min, then exposed to ultraviolet light (light intensity, 15 mW/cm^2) for 45 s, and finally, developed for 1 min in a solution (liquid ratio, AZ 400K: DI water = 1:3). After development, the PR was removed by acetone and rinsed by DI water. Next, the piezoresistive rubbery precursor was screen-printed onto the stretchable electrodes via screen-printing assisted by a laser-cut steel mask (0.3 mm thick, area of 5 mm × 5 mm). After blade-coating the piezoresistive rubbery precursor, the sample along with the steel mask was heated at 150 °C for 45 min until the PZT rubber completely cured. After tearing off the steel mask, the top PDMS encapsulation layer with a thickness of 0.17 mm was spin-coated and cured.

2.3. Characterization

Data presented in Figure 2a,c,d and Figure 3c,f,i were collected under a self-developed oscillator with controllable stress and frequencies, using Keysight B1500A Semiconductor Analyzer (Keysight Technologies, Santa Rosa, CA, USA). Data shown in Figure 2b was collected by finger touching, tapping, and hitting, using Keysight B1500A Semiconductor Analyzer. The complete data acquisition chain is shown in Figure S1. The surface morphology was observed by a field emission scanning electron microscopy (FEI Quanta 450 FESEM, FELMI-ZFE, Graz, Austria). Informed consent was obtained from the volunteers.

3. Results and Discussion

Figure 1a presents a schematic illustration of the graphene/CNT/Ecoflex composite-based strain sensor. It has a multilayered structure where two pieces of thin PDMS layers (thickness, 0.34 mm; PDMS: crosslink, 30:1) serves as the substrate and the encapsulation, and the piezoresistive graphene/CNT/Ecoflex composite in the middle serves as the sensing layer. The blend ratio of the ternary graphene/CNT/Ecoflex was set as 97.98 wt.% Ecoflex, 1.73 wt.% CNT, and 0.29 wt.% graphene (Figure 1b). The conductive electrode adopted a structurally designed copper trace, 6 μm, for collecting strain responses. The sensor is stretchable, reversible, soft, and adhesive to various surfaces, which can be directly laminated on the skin. The overall dimension of the strain sensor is 11.6 mm × 6.3 mm × 0.64 mm. Figure 1c shows the details of the copper electrode of the strain sensor, whose serpentine design can ensure great stretchability in different directions. By integrating the graphene/CNT/Ecoflex composite, the stretchable electrodes and the PDMS encapsulation layers, the entire system owns superb flexibility and stretchability. It is soft enough to be integrated with skin even under stretching, twisting, and squeezing (Figure 1d). Figure 1e presents a scanning electron microscopy (SEM) image of the graphene/CNT/Ecoflex composite where we can observe the uniform and smooth surface.
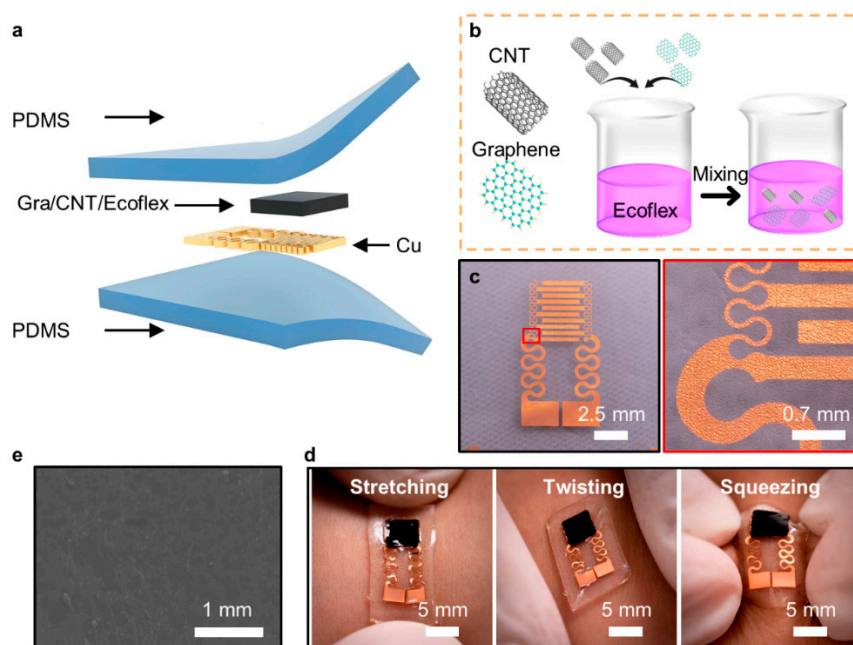

Figure 1. Flexible, skin-integrated strain sensor with a graphene/CNT/Ecoflex composite as a functional layer. (**a**) Schematic illustration of the strain sensor. (**b**) Fabrication process of the graphene/CNT/Ecoflex composite. (**c**) Optical image of the in-plane electrodes (copper), and its enlarged optical image of the electrode pattern. (**d**) Optical image of the strain sensor attached on the skin surface with three mechanical deformations, including stretching, twisting, and squeezing. (**e**) Scanning electron microscope of the surface morphology for the graphene/CNT/Ecoflex composite thin film.

To characterize the performance of the strain sensor, the response ($\Delta R/R_0$) curves versus different parameters are measured and calculated in Figure 2a, where R_0 (measured of 8 Megohm) is the initial resistance before any mechanical loadings, and ΔR is the resistance variations. It is found that the electrical signal raised monotonously when the strain sensor is stretched from 0% to 20% ($\Delta R/R_0$ increase from 0.0144 to 4.856), demonstrating its high sensitivity (the absolute value of the relative resistance change rate induced under one testing unit strain level, 26). Figure 2b presents the electrical signal of the device triggered by finger touching, tapping, and hitting with the electrical signal of 0.0988, 0.32, and 1.1, respectively, exhibiting its ability in distinguishing applied pressure differences. To investigate the electrical stability in converting human motion into electrical signal, we studied relationship between performance and various low frequencies that are relevant to daily body motions, ranging from 0.1 to 0.4 Hz with a constant strain of 5% (Figure 2c). It is found that the low frequency has a negligible effect on the device signal outputs, demonstrating its sufficient response time (~41 ms). Fatigue tests were conducted for the strain sensor that associated with repeated stretching for 80 cycles at 1 Hz (Figure 2d) with the electrical signal ranging from 0 to 1. These results prove that the sensor is stable enough to endure highly intensive stretching motions.
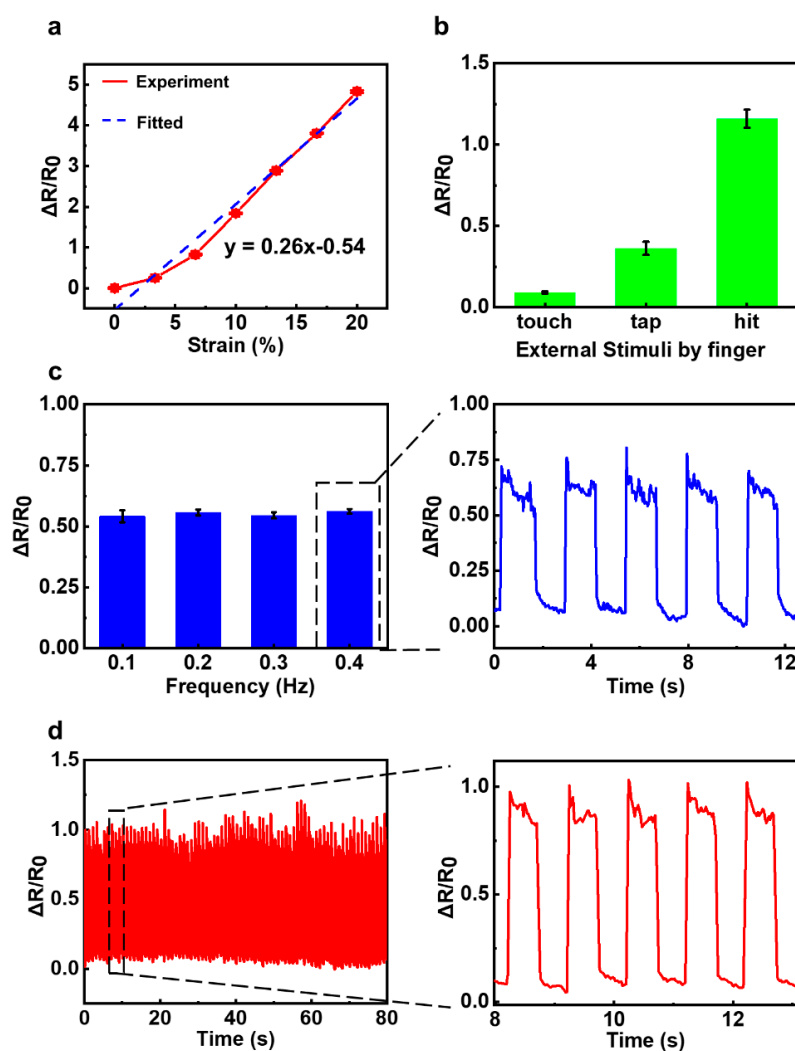

Figure 2. Electrical properties of the graphene/CNT/Ecoflex composite-based strain sensor. (**a**) Electrical signals ($\Delta R/R_o$) of the device at different strain values. (**b**) Electrical signals of the device to three loads (touching, tapping, and hitting). (**c**) Electrical signals of the device under different frequencies under 5% strain. (**d**) Electrical signals of the device in a fatigue test for 80 cycles at a constant frequency of 1 Hz.

To demonstrate the remarkable sensitivity of the strain sensor, a blowing test is conducted as the sensor is mounted on a clean cloth (Figure 3a,b) for recording the blows. The intensity of airflow is ~7.38 standard liter per minute (SLPM), at a frequency of 0.25 Hz. The strain sensor has a clear response to the blowing with the $\Delta R/R_0$ values of 0–0.69 (Figure 3c). To demonstrate its high sensitivity, the sensor was mounted on the neck of a volunteer for detecting the swallowing motion, as shown in Figure 3d,e. The $\Delta R/R_0$ shows a regular variation along with the swallowing motion, ranging from 0 to 0.295 (Figure 3f). Its high sensitivity towards blowing and throat movements demonstrates the potential of the flexible strain sensor in clinical-related applications and many other fields in biomedical engineering. Figure 3g show optical images of a strain sensor mounted on the back of hand, where the index finger is at different bending angles. The electrical signal at the bending angle of 30°, 60°, and 90° are 0.4285, 0.6812, and 2.59, respectively, where the maximum $\Delta R/R_0$ at 90° is 6.19 (Figure 3h,i). It shows that the strain sensor is capable of measuring tiny body motion, and this is applied for further robotic control.
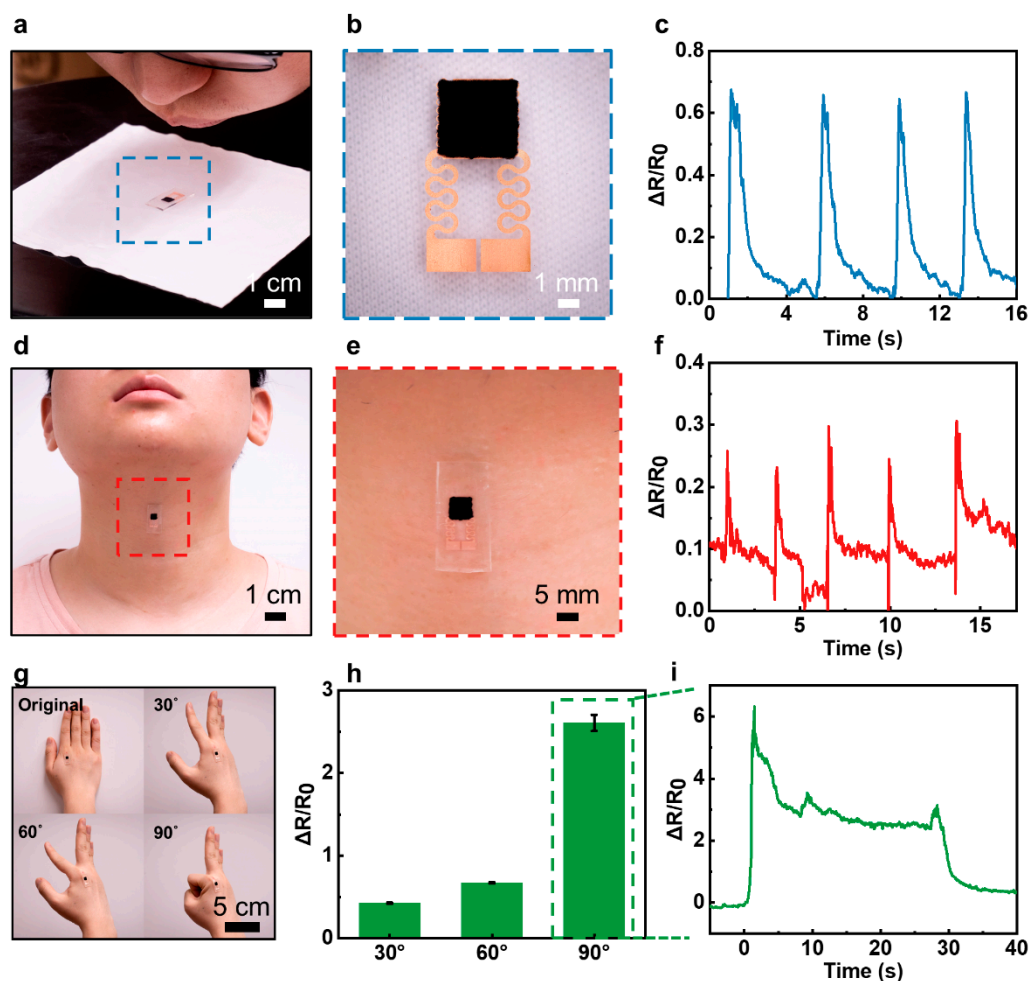

Figure 3. The electrical signals of the flexible strain sensor under different external stimuli. (**a**) Optical image of the flexible strain sensor under human directly blowing. (**b**) An enlarged optical image of the flexible strain sensor. (**c**) Electrical signals of the flexible strain sensor in the blowing test shown in (**a**). (**d**) Optical image of the flexible strain sensor mounted on a throat for a swallow test. (**e**) An enlarged optical image of the flexible strain sensor mounted on a throat. (**f**) Electrical signals of the flexible strain sensor in the swallow test shown in (**d**). (**g**) Optical image of a flexible strain sensor mounted on the back of a hand, and the index finger bending at different angles (original, 30°, 60°, and 90°). (**h**) Electrical signals of the flexible strain sensor under different finger bending angles shown in (**g**). (**i**) Detailed statistics of the measurement at 90° shown in (**h**).

Next, we used the strain sensors for human–machine interfaces with the schematic diagram of testing circuit shown in Figure 4a. To accurately capture hands and fingers motions, sensors were mounted on a rubber glove (Figure 4b). Figure 4c–f shows different gestures (tick, eight, yeah, and okay) created by the tester, and the same gestures are also reproduced by the robotic hand. Figure S2 presents the controlling code with a channel signal. The high sensitivity and accuracy of the sensors lead to smooth control of the robotic hand, and it bends almost without any time delay after the finger bends. Moreover, the robotic fingers could imitate the bending angle of the human hand due to the verifying electrical signals. It is concluded that the strain sensors can control the robotic hand in smooth and natural approach, and the feasibility of applying strain sensors in machine control and human–machine interface is demonstrated.
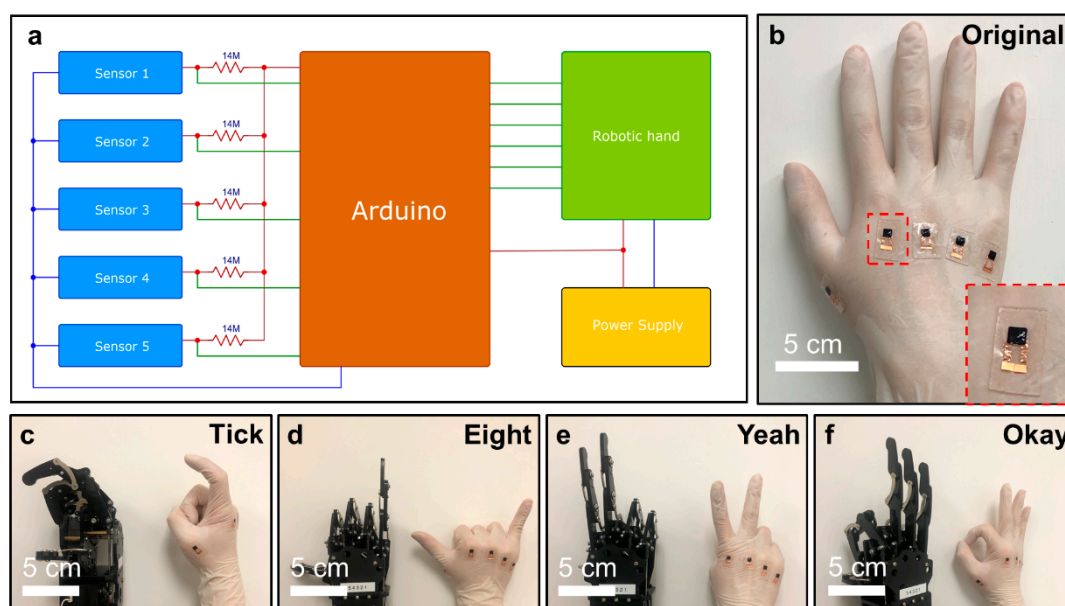

Figure 4. Robotic hand controlling performed by the flexible strain sensors. (**a**) The schematic diagram of the testing circuit for controlling robotic hand. (**b**) Optical image of strain sensors mounted on a rubbery glove. Optical image illustrating that the strain sensors control a robotic hand to make gestures of "tick" (**c**), "eight" (**d**), "yeah" (**e**), "okay" (**f**).

4. Conclusions

In summary, a graphene/CNT/Ecoflex composite-based strain sensor and their applications in human–machine interfaces are introduced in this work. With the advantages of flexible, stretchable, and skin-integrated characteristics, the soft strain sensors could be laminated on human skin surfaces for body activity sensing. The simple processing route can significantly lower the fabrication cost. With experimental integration studies of the ternary-designed flexible strain sensor, we provide a new strategy for intrinsically stretchable sensor development and robotics controlling with a terrific performance. The results presented in this work indicate a new route for developing wearable electronics for human–machine interfaces.

Conflicts of Interest: The authors declare no conflict of interest. The funders had no role in the design of the study; in the collection, analyses, or interpretation of data; in the writing of the manuscript, or in the decision to publish the results.

References

1. Liu, Y.; Zhao, L.; Wang, L.; Zheng, H.; Li, D.; Avila, R.; Lai, K.W.C.; Wang, Z.; Xie, Z.; Zi, Y.; et al. Skin-integrated graphene-embedded lead zirconate titanate rubber for energy harvesting and mechanical sensing. *Adv. Mater. Technol.* **2019**, *4*, 60–63. [CrossRef]

2. Xie, Z.; Avila, R.; Huang, Y.; Rogers, J.A. Flexible and stretchable antennas for biointegrated electronics. *Adv. Mater.* **2020**, *32*, 1–16. [CrossRef] [PubMed]

3. Yu, X.; Xie, Z.; Yu, Y.; Lee, J.; Vazquez-Guardado, A.; Luan, H.; Ruban, J.; Ning, X.; Akhtar, A.; Li, D.; et al. Skin-integrated wireless haptic interfaces for virtual and augmented reality. *Nature* **2019**, *575*, 473–479. [CrossRef]

4. Jeong, Y.R.; Kim, J.; Xie, Z.; Xue, Y.; Won, S.M.; Lee, G.; Jin, S.W.; Hong, S.Y.; Feng, X.; Huang, Y.; et al. A skin-attachable, stretchable integrated system based on liquid GaInSn for wireless human motion monitoring with multi-site sensing capabilities. *NPG Asia Mater.* **2017**, *9*, 1–8. [CrossRef]

5. Liu, Y.; Zhao, L.; Avila, R.; Yiu, C.; Wong, T.; Chan, Y.; Yao, K.; Li, D.; Zhang, Y.; Li, W.; et al. Epidermal electronics for respiration monitoring via thermo-sensitive measuring. *Mater. Today Phys.* **2020**, *13*, 100199. [CrossRef]

6. Wang, Y.; Hao, J.; Huang, Z.; Zheng, G.; Dai, K.; Liu, C.; Shen, C. Flexible electrically resistive-type strain sensors based on reduced graphene oxide-decorated electrospun polymer fibrous mats for human motion monitoring. *Carbon* **2018**, *126*, 360–371. [CrossRef]

7. Lee, Y.; Kim, J.; Hwang, H.; Jeong, S.H. Highly stretchable and sensitive strain sensors based on single-walled carbon nanotube-coated nylon textile. *Korean J. Chem. Eng.* **2019**, *36*, 800–806. [CrossRef]

8. Liu, Y.; Wang, L.; Zhao, L.; Yu, X.; Zi, Y. Recent progress on flexible nanogenerators toward self-powered systems. *InfoMat* **2020**, *2*, 318–340. [CrossRef]

9. Bae, S.H.; Lee, Y.; Sharma, B.K.; Lee, H.J.; Kim, J.H.; Ahn, J.H. Graphene-based transparent strain sensor. *Carbon* **2013**, *51*, 236–242. [CrossRef]

10. Liu, Y.; Pharr, M.; Salvatore, G.A. Lab-on-skin: A review of flexible and stretchable electronics for wearable health monitoring. *ACS Nano* **2017**, *11*, 9614–9635. [CrossRef]

11. Gong, S.; Lai, D.T.H.; Su, B.; Si, K.J.; Ma, Z.; Yap, L.W.; Guo, P.; Cheng, W. Highly stretchy black gold e-skin nanopatches as highly sensitive wearable biomedical sensors. *Adv. Electron. Mater.* **2015**, *1*, 1–7. [CrossRef]

12. He, Z.; Zhou, G.; Byun, J.H.; Lee, S.K.; Um, M.K.; Park, B.; Kim, T.; Lee, S.B.; Chou, T.W. Highly stretchable multi-walled carbon nanotube/thermoplastic polyurethane composite fibers for ultrasensitive, wearable strain sensors. *Nanoscale* **2019**, *11*, 5884–5890. [CrossRef]

13. Wang, L.; Chen, Y.; Lin, L.; Wang, H.; Huang, X.; Xue, H.; Gao, J. Highly stretchable, anti-corrosive and wearable strain sensors based on the PDMS/CNTs decorated elastomer nanofiber composite. *Chem. Eng. J.* **2019**, *362*, 89–98. [CrossRef]

14. Almassri, A.M.M.; Hasan, W.Z.W.; Ahmad, S.A.; Ishak, A.J. A sensitivity study of piezoresistive pressure sensor for robotic hand. In Proceedings of the RSM 2013 IEEE Regional Symposium on Micro and Nanoelectronics, Daerah Langkawi, Malaysia, 25–27 September 2013; pp. 394–397. [CrossRef]

15. Huang, S.; Liu, Y.; Zhao, Y.; Ren, Z.; Guo, C.F. Flexible electronics: Stretchable electrodes and their future. *Adv. Funct. Mater.* **2019**, *29*, 1–15. [CrossRef]

16. Saudabayev, A.; Varol, H.A. Sensors for robotic hands: A survey of state of the art. *IEEE Access* **2015**, *3*, 1765–1782. [CrossRef]

17. Shao, B.; Liu, Y.; Zhuang, X.; Hou, S.; Han, S.; Yu, X.; Yu, J. Crystallinity and grain boundary control of TIPS-pentacene in organic thin-film transistors for the ultra-high sensitive detection of NO_2. *J. Mater. Chem. C* **2019**, *7*, 10196–10202. [CrossRef]

18. Hou, S.; Yu, J.; Zhuang, X.; Li, D.; Liu, Y.; Gao, Z.; Sun, T.; Wang, F.; Yu, X. Phase separation of P3HT/PMMA blend film for forming semiconducting and dielectric layers in organic thin-film transistors for high-sensitivity NO_2 detection. *ACS Appl. Mater. Interfaces* **2019**, *11*, 44521–44527. [CrossRef]

19. Han, S.; Kim, J.; Won, S.M.; Ma, Y.; Kang, D.; Xie, Z.; Lee, K.T.; Chung, H.U.; Banks, A.; Min, S.; et al. Battery-free, wireless sensors for full-body pressure and temperature mapping. *Sci. Transl. Med.* **2018**, *10*. [CrossRef]

20. Wang, X.; Li, J.; Song, H.; Huang, H.; Gou, J. Highly stretchable and wearable strain sensor based on printable carbon nanotube layers/polydimethylsiloxane composites with adjustable sensitivity. *ACS Appl. Mater. Interfaces* **2018**, *10*, 7371–7380. [CrossRef]

21. Yamada, T.; Hayamizu, Y.; Yamamoto, Y.; Yomogida, Y.; Izadi-Najafabadi, A.; Futaba, D.N.; Hata, K. A stretchable carbon nanotube strain sensor for human-motion detection. *Nat. Nanotechnol.* **2011**, *6*, 296–301. [CrossRef]

22. Mahadeva, S.K.; Yun, S.; Kim, J. Flexible humidity and temperature sensor based on cellulose-polypyrrole nanocomposite. *Sens. Actuators A Phys.* **2011**, *165*, 194–199. [CrossRef]

23. Liu, P.; Zhu, R.; Que, R. A flexible flow sensor system and its characteristics for fluid mechanics measurements. *Sensors* **2009**, *9*, 9533–9543. [CrossRef]

24. Shikida, M.; Yoshikawa, K.; Iwai, S.; Sato, K. Flexible flow sensor for large-scale air-conditioning network systems. *Sens. Actuators A Phys.* **2012**, *188*, 2–8. [CrossRef]

25. Li, Y.; Samad, Y.A.; Taha, T.; Cai, G.; Fu, S.; Liao, K. Highly flexible strain sensor from tissue paper for wearable electronics. *ACS Sustain. Chem. Eng.* **2016**, *4*, 4288–4295. [CrossRef]

26. Gong, T.; Zhang, H.; Huang, W.; Mao, L.; Ke, Y.; Gao, M.; Yu, B. Highly responsive flexible strain sensor using polystyrene nanoparticle doped reduced graphene oxide for human health monitoring. *Carbon* **2018**, *140*, 286–295. [CrossRef]

27. Lu, N.; Kim, D.H. Flexible and stretchable electronics paving the way for soft robotics. *Soft Robot.* **2014**, *1*, 53–62. [CrossRef]

28. Zhang, H.; Tao, X. From wearable to aware: Intrinsically conductive electrotextiles for human strain/stress sensing. In Proceedings of the 2012 IEEE-EMBS International Conference on Biomedical and Health Informatics, Hong Kong, China, 5–7 January 2012; pp. 468–471. [CrossRef]

29. Liu, Y.; Wang, L.; Zhao, L.; Yao, K.; Xie, Z.; Zi, Y.; Yu, X. Thin, skin-integrated, stretchable triboelectric nanogenerators for tactile sensing. *Adv. Electron. Mater.* **2020**, *6*, 1901174. [CrossRef]

30. Liu, N.; Chortos, A.; Lei, T.; Jin, L.; Kim, T.R.; Bae, W.G.; Zhu, C.; Wang, S.; Pfattner, R.; Chen, X.; et al. Ultratransparent and stretchable graphene electrodes. *Sci. Adv.* **2017**, *3*, e1700159. [CrossRef] [PubMed]

31. Li, X.; Zhang, R.; Yu, W.; Wang, K.; Wei, J.; Wu, D.; Cao, A.; Li, Z.; Cheng, Y.; Zheng, Q.; et al. Stretchable and highly sensitive graphene-on-polymer strain sensors. *Sci. Rep.* **2012**, *2*, 1–6. [CrossRef]

32. Zhang, S.; Zhang, H.; Yao, G.; Liao, F.; Gao, M.; Huang, Z.; Li, K.; Lin, Y. Highly stretchable, sensitive, and flexible strain sensors based on silver nanoparticles/carbon nanotubes composites. *J. Alloys Compd.* **2015**, *652*, 48–54. [CrossRef]

33. Krantz, J.; Stubhan, T.; Richter, M.; Spallek, S.; Litzov, I.; Matt, G.J.; Spiecker, E.; Brabec, C.J. Spray-coated silver nanowires as top electrode layer in semitransparent P3HT:PCBM-based organic solar cell devices. *Adv. Funct. Mater.* **2013**, *23*, 1711–1717. [CrossRef]

34. Li, Y.; Shang, Y.; He, X.; Peng, Q.; Du, S.; Shi, E.; Wu, S.; Li, Z.; Li, P.; Cao, A. Overtwisted, resolvable carbon nanotube yarn entanglement as strain sensors and rotational actuators. *ACS Nano* **2013**, *7*, 8128–8135. [CrossRef]

35. Liu, L.; Ma, W.; Zhang, Z. Macroscopic carbon nanotube assemblies: Preparation, properties, and potential applications. *Small* **2011**, *7*, 1504–1520. [CrossRef]

36. Yu, S.; Wang, X.; Xiang, H.; Zhu, L.; Tebyetekerwa, M.; Zhu, M. Superior piezoresistive strain sensing behaviors of carbon nanotubes in one-dimensional polymer fiber structure. *Carbon* **2018**, *140*, 1–9. [CrossRef]

37. Zheng, Y.; Li, Y.; Li, Z.; Wang, Y.; Dai, K.; Zheng, G.; Liu, C.; Shen, C. The effect of filler dimensionality on the electromechanical performance of polydimethylsiloxane based conductive nanocomposites for flexible strain sensors. *Compos. Sci. Technol.* **2017**, *139*, 64–73. [CrossRef]

38. Liu, C.X.; Choi, J.W. Patterning conductive PDMS nanocomposite in an elastomer using microcontact printing. *J. Micromech. Microeng.* **2009**, *19*. [CrossRef]

39. Zhou, J.; Xu, X.; Xin, Y.; Lubineau, G. Coaxial thermoplastic elastomer-wrapped carbon nanotube fibers for deformable and wearable strain sensors. *Adv. Funct. Mater.* **2018**, *28*, 1–8. [CrossRef]

40. Li, Q.; Li, J.; Tran, D.; Luo, C.; Gao, Y.; Yu, C.; Xuan, F. Engineering of carbon nanotube/polydimethylsiloxane nanocomposites with enhanced sensitivity for wearable motion sensors. *J. Mater. Chem. C* **2017**, *5*, 11092–11099. [CrossRef]

41. Zhang, R.; Ying, C.; Gao, H.; Liu, Q.; Fu, X.; Hu, S. Highly flexible strain sensors based on polydimethylsiloxane/carbon nanotubes (CNTs) prepared by a swelling/permeating method and enhanced sensitivity by CNTs surface modification. *Compos. Sci. Technol.* **2019**, *171*, 218–225. [CrossRef]

42. Filippidou, M.K.; Tegou, E.; Tsouti, V.; Chatzandroulis, S. A flexible strain sensor made of graphene nanoplatelets/polydimethylsiloxane nanocomposite. *Microelectron. Eng.* **2015**, *142*, 7–11. [CrossRef]